Analytica Chimica Acta 853 (2015) 495–500

Contents lists available at ScienceDirect

Analytica Chimica Acta

journal homepage: www.elsevier.com/locate/aca

Rolling cycle amplification based single-color quantum dots–ruthenium complex assembling dyads for homogeneous and highly selective detection of DNA

Chen Su, Yufei Liu, Tai Ye, Xia Xiang, Xinghu Ji **, Zhike He *

Key Laboratory of Analytical Chemistry for Biology and Medicine (Ministry of Education), College of Chemistry and Molecular Sciences, Wuhan University, Wuhan 430072, PR China

HIGHLIGHTS

- The single-color QDs–Ru assembling dyads were applied in homogeneous DNA assay.
- This biosensor exhibited high selectivity against base mismatched sequences.
- This biosensor could be severed as universal platform for the detection of ssDNA.
- This sensor could be used to detect the target in human serum samples.
- This DNA sensor had a good selectivity under the interference of other dsDNA.

GRAPHICAL ABSTRACT

A universal, label-free, homogeneous, highly sensitive, and selective fluorescent biosensor for DNA detection is developed by using rolling-circle amplification (RCA) based single-color quantum dots–ruthenium complex (QDs–Ru) assembling dyads.

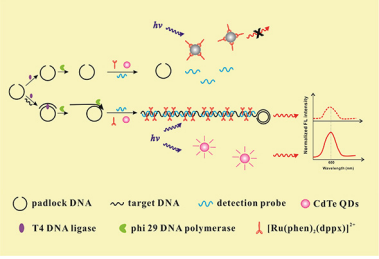

ARTICLE INFO

Article history:
Received 9 July 2014
Received in revised form 11 October 2014
Accepted 15 October 2014
Available online 18 October 2014

Keywords:
DNA detection
Quantum dots
Ruthenium complex
Rolling circle amplification
Signal amplification

ABSTRACT

In this work, a new, label-free, homogeneous, highly sensitive, and selective fluorescent biosensor for DNA detection is developed by using rolling-circle amplification (RCA) based single-color quantum dots–ruthenium complex (QDs–Ru) assembling dyads. This strategy includes three steps: (1) the target DNA initiates RCA reaction and generates linear RCA products; (2) the complementary DNA hybridizes with the RCA products to form long double-strand DNA (dsDNA); (3) $[Ru(phen)_2(dppx)]^{2+}$ (dppx = 7,8-dimethyldipyrido [3,2-a:2′,3′-c] phenanthroline) intercalates into the long dsDNA with strong fluorescence emission. Due to its strong binding propensity with the long dsDNA, $[Ru(phen)_2(dppx)]^{2+}$ is removed from the surface of the QDs, resulting in restoring the fluorescence of the QDs, which has been quenched by $[Ru(phen)_2(dppx)]^{2+}$ through a photoinduced electron transfer process and is overlaid with the fluorescence of dsDNA bonded Ru(II) polypyridyl complex (Ru-dsDNA). Thus, high fluorescence intensity is observed, and is related to the concentration of target. This sensor exhibits not only high sensitivity for hepatitis B virus (HBV) ssDNA with a low detection limit (0.5 pM), but also excellent selectivity in the complex matrix. Moreover, this strategy applies QDs–Ru assembling dyads to the detection of single-strand DNA (ssDNA) without any functionalization and separation techniques.

* Corresponding author. Tel.: +86 27 68756557; fax: +86 27 68754067.
** Corresponding author.
E-mail address: zhkhe@whu.edu.cn (Z. He).

http://dx.doi.org/10.1016/j.aca.2014.10.027
0003-2670/

1. Introduction

Sensitive and selective detection of sequence-specific DNA has attracted increasing attention owing to its potential applicability ranging from genetic research of diseases to clinical diagnosis and therapy [1–3]. Up to now, many nanomaterials have been exploited for the detection of DNA due to the unique electronic and optical properties, such as quantum dots (QDs) [4], gold nanoparticles [5], silver nanoparticles [6], graphene [7], and so on.

Among these nanomaterials, QDs have been widely employed in various fields as a promising fluorescence probes, mainly fluoroimmunoassays [8], biochemical detections [9], biomedicine imaging [10], and drug delivery [11]. Compared to conventional organic dyes, QDs have superior properties, such as photostability, broad excitation spectra coupled to narrow, symmetric, and tunable emission spectra [12]. Also, a series of QDs-based DNA biosensors have been developed based on fluorescence resonance energy transfer (FRET) [13–16].

As the most classical DNA "light switch" complex, Ru(II) polypyridyl complex can exhibit strong luminescence when it intercalates into double-strand DNA (dsDNA) with strong affinity, but almost nonemissive in dsDNA-free aqueous buffer [17–19]. According to the previous study, Ru(II) polypyridyl complex can quench the fluorescence of QDs through a photoinduced electron transfer process [8]. In the presence of dsDNA, Ru(II) polypyridyl complex is removed away from QDs, producing free QDs and dsDNA bonded Ru(II) polypyridyl complex (Ru-dsDNA). Both of them can be simultaneously excited and emit fluorescence. Based on these phenomena, our group has developed a series of dual-color dyads based fluorescent biosensors for dsDNA detection [20] and protein detection [21] via the use of the red fluorescence of Ru-dsDNA complex and the green fluorescence of QDs. The limit of detection (LOD) of those works are listed in Table S1. In order to obtain the higher sensitivity, Xie's group has developed a novel single-color fluorescence "off-on" switch system for the detection of dsDNA composed of the QDs and $[Ru(phen)_2(dppz)]^{2+}$ (phen = 1,10-phenanthroline, dppz = dipyrido [3,2-a:2′,3′-c] phenazine) (QDs–Ru) assembling dyads [22]. Both of $[Ru(phen)_2(dppz)]^{2+}$ and QDs would emit overlaid fluorescence in the presence of dsDNA, resulting higher fluorescence intensity. This method can get a lower detection limit compared with the dual-color fluorescent sensor, but it is failure for sequence-specific single-strand DNA (ssDNA) detection directly. Furthermore, it is also difficult for those QDs–Ru assembling dyads based biosensors to directly detect the target in relatively complex biological matrix [23–25]. To improve the application limitations of QDs–Ru assembling dyads, functionalized material magnetic microparticles (MMPs) coupled with QDs–Ru dyads have been proposed to direct ssDNA detection with satisfactory results in complex biological matrix [26], however, it is costly and complicated because of its functionalization, separation, and non-homogeneous processes involved. Therefore, it is necessary to develop a new, simple, sensitive, and selective QDs–Ru dyads based strategy for the detection of ssDNA, which can be also achieved homogeneously in complex environment.

Herein, we report rolling-circle amplification (RCA) based single-color QDs–Ru assembly dyads for simple, label free, and homogeneous detection of sequence-specific DNA. Single-color fluorescence, which is obtained from the overlaid fluorescence of Ru-dsDNA and QDs, can greatly improve the sensitivity and get a lower detection limit compared with the dual-color fluorescent sensor. RCA, a simple, reliable and isothermal amplification method, is driven by DNA polymerase to generate a long tandem repeat product based on a circular DNA template, without advanced laboratory equipment or experimental expertise [27–29]. In the presence of the complementary strand, the RCA products form long dsDNA with thousands of repeated units. At the same time, the low background can be achieved without hairpin in RCA. With the aid of RCA, this QDs–Ru dyads based biosensor shows a high sensitive and selective performance to the ssDNA detection over the range from 3.3 to 27 pM with a detection limit of 0.5 pM. Meanwhile, this method can be applied in complex environment without any separation techniques.

2. Materials and methods

2.1. Reagents and apparatus

T4 DNA ligase and dNTPs were obtained from Takara Biotechnology (Dalian) Co., Ltd. (China). Phi 29 DNA polymerase was purchased from New England Biolabs (England). Bovine serum albumin (BSA) was obtained from Roche (USA). Tris(hydroxymethyl) aminomethane hydrochloride (tris) was purchased from Sigma–Aldrich (USA). The human serum sample was supplied by Zhongnan Hospital of Wuhan University. All of the other reagents were of analytical-reagent grade or better, and the water used to prepare buffer solutions was prepared by a Milli-Q water system (Millipore Corp., USA) with resistivity of 18.2 MΩ cm. DNA oligonucleotides with different sequences were synthesized and HPLC purified by Sangon Biotechnology Co., Ltd. (China). The sequences of the oligonucleotides used in this study are as follows:

- Padlock probe: 5′-phosphate ATAACTGAAAGC-CAATTCTTGTTTCCTTTCCTTGAAACTTCTTTCTTTCTT 3CCTCGTAC-CACTACATCCAT-3′;
- 1HBV DNA: 5′-TTGGCTTTCAGTTATATGGATGTAGTGGTA-3′;
- Detection probe: 5′-AGCCAATTCTTGTTTCCTTTCCTT-GAAACTTCTTTCTTTCTTCCTCGTACCAC-3′;
- Mismatch DNA 1: 5′-TTGGCTTTCAGTTATTTGGATGTAGTGGTA-3′;
- Mismatch DNA 2: 5′-TTGGCTTTCAATTATTTGGATGTAGTGGTA-3′;
- Mismatch DNA 3: 5′-TTGGCTTTCAATTATTTTGATGTAGTGGTA-3′;
- Interferential DNA 1: 5′-CTGTTCGCGCTGGTCATG-3′;
- Interferential DNA 2: 5′-CATGACCAGCGCGAACAG-3′.

Fluorescence spectra were obtained with a RF-5301PC spectrophotometer (Shimadzu, Japan) equipped with a 150 W xenon lamp (Ushio Inc., Japan). UV–vis spectra were recorded on a UV-2550 spectrometer (Shimadzu, Japan). Gels were imaged by a ChemiDoc XRD system (Bio-Rad USA).

2.2. Preparation of $Ru(phen)_2(dppx)^{2+}$ and CdTe QDs

The synthesis of $[Ru(phen)_2(dppx)]^{2+}$ (dppx = 7,8-dimethyldipyrido [3,2-a:2′,3′-c] phenanthroline) and water-soluble *N*-acetylcysteine (NAC)-capped CdTe QDs were performed according to previous reports [30,31]. The stock solution of $[Ru(phen)_2(dppx)]^{2+}$ (0.1 mM) was prepared in ultrapure water. The QDs (7.7 mM) were dissolved in Tris–HCl buffer solution (10 mM, pH 8.0) for further experiments.

2.3. Amplified detection of target DNA

Firstly, 5 μL of 0.1 μM padlock probe DNA and different concentrations of the targets were added in 40 μL of ligation buffer solution (30 mM Tris–HCl, 10 mM $MgCl_2$, 1 mM ATP, pH 7.8), Then, 50 U of T4 DNA ligase was added and the mixture was incubated at 37 °C for 2 h to complete the ligation of padlock probe. After ligation, T4 DNA ligase was inactivated by heating the

reaction mixture at 65 °C for 10 min. The resulting circular DNA could be used directly or stored at 20 °C.

Secondly, 10 μL of the circular DNA, 10 U of the phi 29 DNA polymerase, 2 μL of 10 mg mL^{-1} BSA and 2 μL of 10 mM dNTPs were mixed to a final volume of 100 μL in polymerase buffer (50 mM Tris–HCl, 10 mM $MgCl_2$, 10 mM $(NH_4)_2SO_4$, pH 7.5). After incubating at 37 °C for 3 h, detection probe (3 nM) was added.

Finally, 10 μL of the hybridized solution, 14 μL of 0.1 mM [Ru(phen)$_2$(dppx)]$^{2+}$ and 30 μL of 7.7 μM QDs were mixed to a final volume of 300 μL in the Tris–HCl buffer. After incubating 15 min, the fluorescence signal was measured with fluorescence spectrometry. Excitation wavelength was 388 nm and the scan range was from 500 to 700 nm. All measurements were done in triplicate.

3. Results and discussions

3.1. Design of the amplified biosensor

RCA, as an advanced DNA amplified technique alternative to PCR, was applied to construct RCA-based QDs–Ru assembling dyads for ssDNA biosensor. In this work, HBV gene oligonucleotide sequence was used as a model. As illustrated in Fig. 1, in the presence of target, when the 3′ and the 5′- ends of the padlock probe were perfectly hybridized to the target sequence, the linear padlock probe could be specifically ligated by T4 DNA ligase and formed a circular DNA. This circular DNA could subsequently be used as the template of RCA. In the presence of dNTPs, target DNA hybridized with this circular template and was subsequently amplified by phi 29 DNA polymerase. Thus, the RCA reaction was initiated to produce a long single-stranded RCA product with thousands of repeated units. After the addition of the detection probes, a long dsDNA was formed due to the hybridization of probes with RCA products. Then a large number of [Ru(phen)$_2$(dppx)]$^{2+}$ intercalated into the long dsDNA and QDs fluorescence was restored with an emission peak at 600 nm, which was almost overlaid with the fluorescence of Ru-dsDNA. In the absence of the target, no RCA products were formed so that the QDs fluorescence was quenched by [Ru(phen)$_2$(dppx)]$^{2+}$ with low fluorescence intensity. By monitoring the fluorescence signal, the concentration of the target could be determined.

3.2. The verification of RCA reaction

In order to prove the RCA products, the electrophoresis experiments were performed. As shown in Fig. S1, compared with DNA marker in lane M, no RCA products could be observed in the absence of the target (lane 3) or phi 29 DNA polymerase (lane 2). Only the reaction system containing the target and phi 29 DNA polymerase showed a bright electrophoresis band (lane 1), demonstrating the formation of long DNA products.

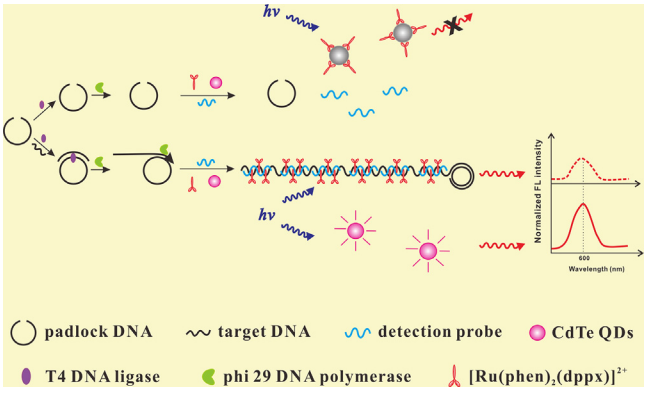

Fig. 1. Schematic demonstration of the amplified biosensor for DNA detection.

3.3. The feasibility of the amplification strategy

To demonstrate the feasibility of the amplification DNA sensor, the feasible experiment has been carried out. From the results shown in Fig. 2, we could see a weak fluorescent emission (curve b) in the absence of target due to the fluorescence quenching of QD by [Ru(phen)$_2$(dppx)]$^{2+}$. However, the hybridization of target (without phi 29 DNA polymerase) with the padlock probe led to a small increase in fluorescence intensity (curve d). Importantly, when phi 29 DNA polymerase was added, a significant increase in fluorescence intensity was observed (curve e). Such increase was due to the fact that the existence of target and phi 29 DNA polymerase triggered the RCA, leading to a strong overlaid fluorescence of the RCA products bonded [Ru(phen)$_2$(dppx)]$^{2+}$ and QDs. Furthermore, it was obvious that the difference of the fluorescence intensity after the addition of target was gradually reduced without QDs (curve a, c). These results indicated that this amplification strategy for DNA detection via RCA and single-color QDs–Ru assembling dyads was feasible.

3.4. The effective quenching of QDs fluorescence by [Ru(phen)$_2$(dppx)]$^{2+}$

We further explored the quenching effect of [Ru(phen)$_2$(dppx)]$^{2+}$ on QDs. A range of concentrations of [Ru(phen)$_2$(dppx)]$^{2+}$ were investigated as shown in Fig. S2(A). The fluorescence intensity of QDs gradually decreased with increasing concentration of [Ru(phen)$_2$(dppx)]$^{2+}$. The quenching behavior of [Ru(phen)$_2$(dppx)]$^{2+}$ on the fluorescence of QDs was found to follow a conventional Stern–Volmer relationship:

$$\frac{I_0}{I} = 1 + K_{SV}[M] \quad (1)$$

where I_0 and I are the fluorescence intensities of QDs in the absence and presence of [Ru(phen)$_2$(dppx)]$^{2+}$; [M] is the concentration of

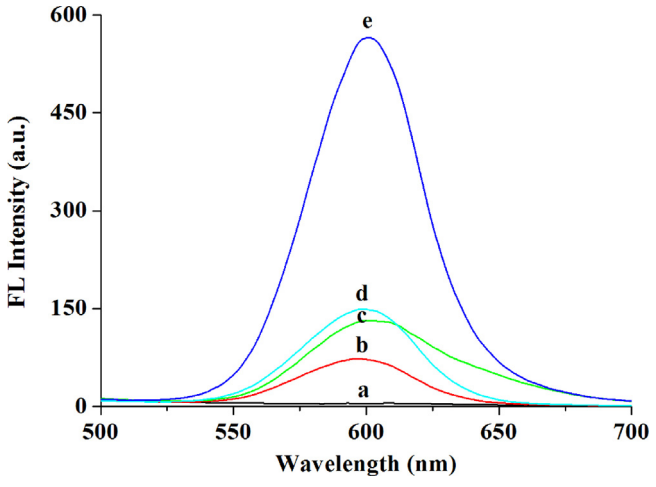

Fig. 2. Fluorescence responses of the biosensor with (a): phi 29 DNA polymerase and [Ru(phen)$_2$(dppx)]$^{2+}$; (b): phi 29 DNA polymerase, [Ru(phen)$_2$(dppx)]$^{2+}$ and QDs; (c): target, [Ru(phen)$_2$(dppx)]$^{2+}$ and QDs; (d): target, phi 29 DNA polymerase and [Ru(phen)$_2$(dppx)]$^{2+}$; (e): target, phi 29 DNA polymerase, [Ru(phen)$_2$(dppx)]$^{2+}$ and QDs. Experimental conditions: [Ru(phen)$_2$(dppx)]$^{2+}$, 4.7 μM; QDs, 0.77 μM; padlock probe, 33 pM; target DNA, 33 pM; T4 DNA ligase, 50 U; phi 29 DNA polymerase, 6 U; detection probe, 3 nM.

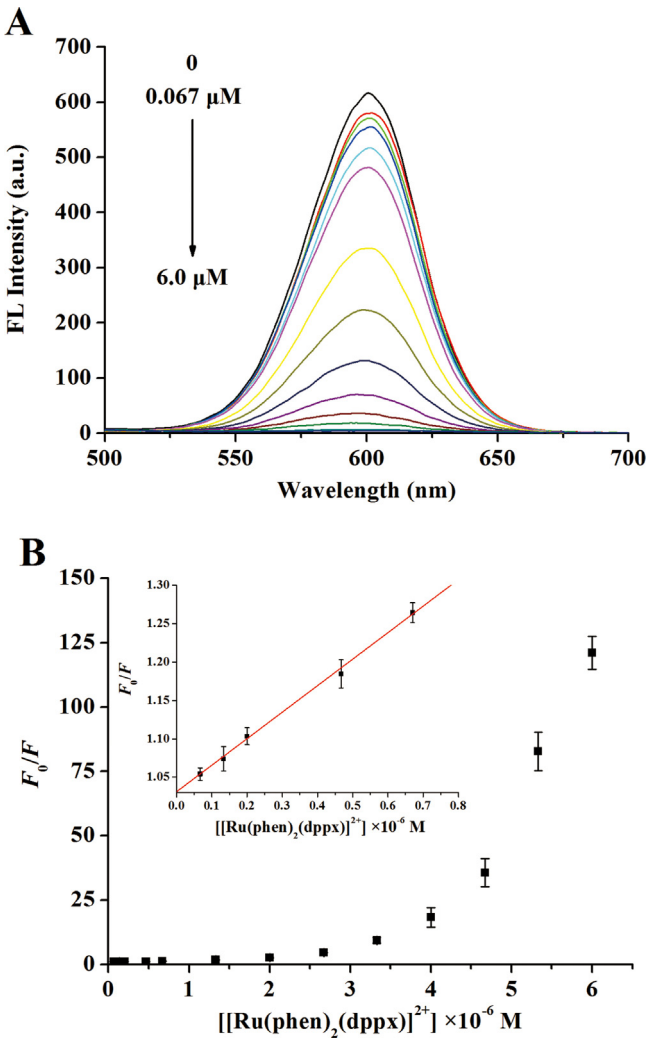

Fig. 3. The fluorescence "off-on" system for DNA detection. (A) Changes in the fluorescence spectra of the QDs and $[Ru(phen)_2(dppx)]^{2+}$ upon the addition of increasing concentrations of the target: 0, 3.3, 6.7, 13, 20, 27, 33 pM, respectively. (B) The fluorescence intensity vs the concentrations of the target, inset: linear relationship between the $F–F_0$ (increased fluorescence intensity) and the concentrations of the target.

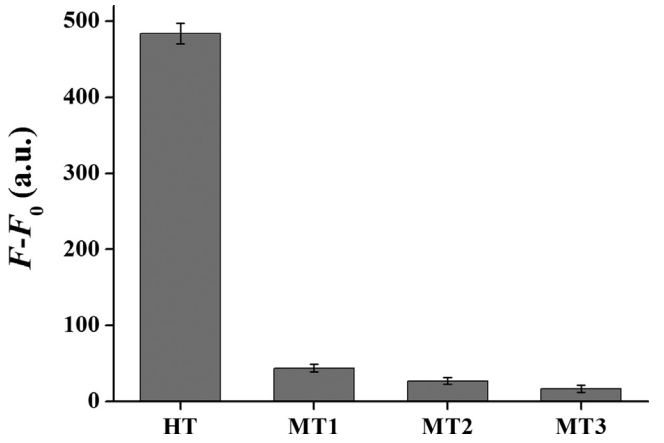

Fig. 4. The $F–F_0$ (increased fluorescence intensity) histogram of the sensing system including 33 pM of the complementary target HT, single-base mismatched target (MT1), two-base mismatched target (MT2) and three-base mismatched target (MT3).

$[Ru(phen)_2(dppx)]^{2+}$; K_{sv} is the quenching constant which defines the quenching efficiency of $[Ru(phen)_2(dppx)]^{2+}$. As shown Fig. S2 (B) inset, the K_{sv} was $3.45 \times 10^7\ M^{-1}$, and the linear range was from 6.7×10^{-8} to 6.7×10^{-7} M. When the concentration of the QDs was 0.77 μM, 4.7 μM $[Ru(phen)_2(dppx)]^{2+}$ was needed to almost completely quench the fluorescence (fluorescence quenching efficiency: 97.0%). To obtain a good response sensitivity of the biosensor, 4.7 μM $[Ru(phen)_2(dppx)]^{2+}$ was chosen in the following experiments.

3.5. Optimization of the RCA reaction conditions

In order to achieve an optimal experimental result, we have investigated the effect of various experimental conditions including the activity of phi 29 DNA polymerase and RCA reaction time. The influence of the activity of phi 29 DNA polymerase used in assay on the fluorescence intensity was shown in Fig. S3. With the increasing activity of phi 29 DNA polymerase, the fluorescence increased at first and then decreased gradually after reaching a plateau at 6 U. The reason might be the increase of background when the activity of phi 29 DNA polymerase was greater than 8 U. Further, we studied the fluorescence signals at different RCA reaction times in the presence of 6 U phi 29 DNA polymerase. As the results shown in Fig. S4, it was observed that the $(F-F_0)$ was increased progressively with the increase of the RCA reaction time when the time was less than 3 h, and then reached a plateau after 3 h. The performance of this assay was dependent on the products of the RCA reaction. In order to achieve the higher detection sensitivity, the longer time was needed to produce enough dsDNA. Meanwhile, the reproducibility of this assay was also subject to the activities of the phi 29 polymerse, such longer time was certainly needed to make sure the completely reaction. Therefore, 6 U of phi 29 DNA polymerase and 3 h as the reaction time were chosen in all the following experiments.

3.6. Quantitative measurement of HBV DNA

To assess the sensitivity of this strategy, quantitative analysis was performed by monitoring the fluorescence of QDs and Ru-dsDNA under the optimized conditions. From Fig. 3A, it could be seen that with increasing concentration of HBV DNA, the intensity of the fluorescence signal increased gradually. By plotting $(F–F_0)$ versus the concentration of HBV DNA ranging from 3.3 to 27 pM, a good linear relationship was obtained (inset of Fig. 3B). The linear equation was $y = 181.0877 \times -9.2385$ with a LOD as low as 0.5 pM (3σ,$n = 9$). The detection sensitivity of this work was comparable to those of the existing signal amplification DNA detection methods [32–34]. Moreover, the LOD could be further improved simply by decreasing the amount of the QDs used in the QDs–Ru assembling dyads formation [22].

3.7. The specificity of biosensor

The specificity of the proposed detection method was further investigated by using four kinds of DNA sequences, including complementary target DNA (HT), single-base mismatched DNA (MT1), two-base mismatched DNA (MT2), and three-base mismatched DNA (MT3) at the same concentration. As shown in Fig. 4, the addition of the mismatched DNA targets only led to a very slight increase in fluorescence intensity. Thus, this method exhibited a good performance to discriminate perfect complementary target and the base mismatched targets. Result showed

Table 1
Determination of the target in 1% human serum with this amplification strategy ($n = 3$).

Sample number	Added (pM)	Found (pM)	Recovery (%)	RSD (%)
1	10.00	11.22	112.2	10.8
2	13.33	12.33	92.5	7.8
3	16.67	15.53	93.2	9.0
4	20.00	18.54	92.7	14.0
5	26.67	27.36	102.6	8.9

that it provided a great opportunity for single-nucleotide polymorphism analysis.

3.8. Determination of target in complex matrix

We further challenged the detection toward the target in relatively complex biological matrix. As the serum with high concentration influenced the photoinduced electron transfer process between $[Ru(phen)_2(dppx)]^{2+}$ and QDs which reduced the sensitivity of this strategy. This strategy could be applied in the complex matrix with a high serum percentage by diluting the complex matrix. Dilution to 1% was chosen in this work. Different concentrations of target were added into 1% human serum samples. The recovery of the target detected by the amplified sensor in serum samples ranged from 92.5 to 112.2%, which were satisfactory for quantitative assays performed in biological samples (Table 1). Finally, we tested the interference rejection of this amplification strategy. As shown in Fig. 5, the fluorescence intensity remained basically unchanged in the presence of interferential dsDNA. As containing large amount of bases, the long RCA product had a much stronger binding propensity with the Ru(II) polypyridyl complex than the interferential dsDNA, even when the concentration of the interferential dsDNA was 100 times higher than the target in this work. For this reason, this single-color sensor had a good selectivity of interferential dsDNA in a certain range of concentrations. These results indicated the potentiality of the proposed assay for DNA detection in complex matrix.

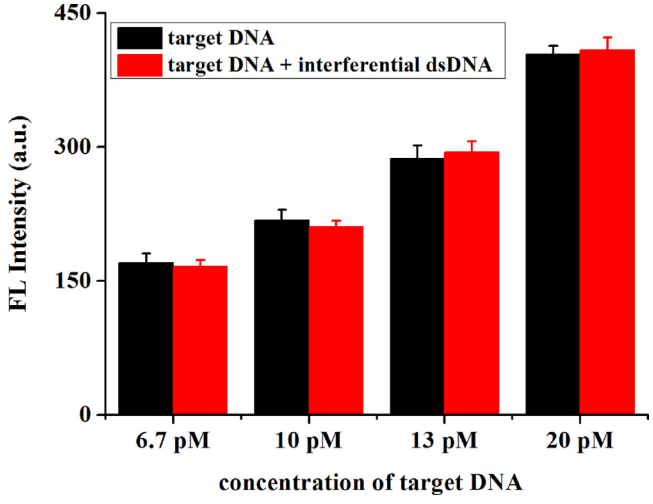

Fig. 5. Comparison of the fluorescence intensity in the absence (black bar)/presence (red bar) of interferential dsDNA (100 fold concentration of the target) upon the addition of increasing concentrations of the target. (For interpretation of the references to color in this figure legend, the reader is referred to the web version of this article)

4. Conclusions

In conclusion, we have successfully developed a new, label-free, homogeneous, highly sensitive, and selective fluorescent biosensor for DNA detection via the use of RCA based single-color QDs–Ru assembling dyads. Taking the HBV DNA as a model analyte, the target is detected in a range from 3.3 to 33 pM with a low LOD (0.5 pM). This sensor not only has high selectivity against single-, two- and three-base mismatched sequences owing to the introduction of RCA, but also can be used to detect the target in 1% human serum samples with satisfactory results, and keep feasibility under the interference of other dsDNA. In addition, it will be expanded to detect a wide range of DNAs in general with a rational design of the corresponding DNA sequences. In view of these advantages, this amplified fluorescent DNA biosensor has a great potential in the area of disease diagnostics and clinical analysis.

Acknowledgments

This work was supported by the National Key Scientific Program-Nanoscience and Nanotechnology (2011CB933600), the National Science Foundation of China (21275109 and 21205089) and Suzhou Nanotechnology Special Project(ZXG2013028).

Appendix A. Supplementary data

Supplementary data associated with this article can be found, in the online version, at http://dx.doi.org/10.1016/j.aca.2014.10.027.

References

[1] J. Wang, Survey and summary from DNA biosensors to gene chips, Nucleic Acids Res. 28 (2000) 3011–3016.
[2] N.L. Rosi, C.A. Mirkin, Nanostructures in biodiagnostics, Chem. Rev. 105 (2005) 1547–1562.
[3] G. Liu, Y. Wan, V. Gau, J. Zhang, L.H. Wang, S.P. Song, C.H. Fan, An enzyme-based E-DNA sensor for sequence-specific detection of femtomolar DNA targets, J. Am. Chem. Soc. 130 (2008) 6820–6825.
[4] E. Sharon, R. Freeman, I. Willner, CdSe/ZnS quantum dots-G-quadruplex/hemin hybrids as optical DNA sensors and aptasensors, Anal. Chem. 82 (2010) 7073–7077.
[5] S.P. Song, Z.Q. Liang, J. Zhang, L.H. Wang, G.X. Li, C.H. Fan, Gold-nanoparticle-based multicolor nanobeacons for sequence-specific DNA analysis, Angew. Chem. Int. Ed. 48 (2009) 8670–8674.
[6] F.L. Gao, J.P. Lei, H.X. Ju, Label-free surface-enhanced raman spectroscopy for sensitive DNA detection by DNA-mediated silver nanoparticle growth, Anal. Chem. 85 (2013) 11788–11793.
[7] N. Mohanty, V. Berry, Graphene-based single-bacterium resolution biodevice and DNA transistor: interfacing graphene derivatives with nanoscale and microscale biocomponents, Nano Lett. 8 (2008) 4469–4476.
[8] L. Chen, X.W. Zhang, G.H. Zhou, X. Xiang, X.H. Ji, Z.H. Zheng, Z.K. He, H.Z. Wang, Simultaneous determination of human enterovirus 71 and coxsackievirus B3 by dual-color quantum dots and homogeneous immunoassay, Anal. Chem. 84 (2012) 3200–3207.
[9] C.P. Huang, Y.K. Li, T.M. Chen, A highly sensitive system for urea detection by using CdSe/ZnS core-shell quantum dots, Biosens. Bioelectron. 22 (2007) 1835–1838.
[10] Y. He, Y.L. Zhong, Y.Y. Su, Y.M. Lu, Z.Y. Jiang, F. Peng, T.T. Xu, S. Su, Q. Huang, C.H. Fan, S.T. Lee, Water-dispersed near-infrared-emitting quantum dots of ultrasmall sizes for in vitro and in vivo imaging, Angew. Chem. Int. Ed. 50 (2011) 5695–5698.
[11] D. Li, G. Li, W. Guo, P. Li, E. Wang, J. Wang, Glutathione-mediated release of functional plasmid DNA from positively charged quantum dots, Biomaterials 29 (2008) 2776–2782.
[12] R. Freeman, X.Q. Liu, I. Willner, Amplified multiplexed analysis of DNA by the exonuclease III-catalyzed regeneration of the target DNA in the presence of functionalized semiconductor quantum dots, Nano Lett. 11 (2011) 4456–4461.
[13] D. Zhao, W.H. Chan, Z.K. He, T. Qiu, Quantum dot–ruthenium complex dyads: recognition of double-strand DNA through dual-color fluorescence detection, Anal. Chem. 81 (2009) 3537–3543.

[14] G.X. Jiang, A.S. Susha, A.A. Lutich, F.D. Stefani, J. Feldmann, A.L. Rogach, Cascaded FRET in conjugated polymer/quantum dot/dye-labeled DNA complexes for DNA hybridization detection, ACS Nano 3 (2009) 4127–4131.
[15] H.F. Dong, W.C. Gao, F. Yan, H.X. Ji, H.X. Ju, Fluorescence resonance energy transfer between quantum dots and graphene oxide for sensing biomolecules, Anal. Chem. 82 (2010) 5511–5517.
[16] V. Biju, A. Anas, H. Akita, E.S. Shibu, T. Itoh, H. Harashima, M. Ishikawa, FRET from quantum dots to photodecompose undesired acceptors and report the condensation and decondensation of plasmid DNA, ACS Nano 6 (2012) 3776–3788.
[17] M.S. Choi, M. Yoon, J.O. Baeg, J. Kim, Label-free dual assay of DNA sequences and potassium ions using an aptamer probe and a molecular light switch complex, Chem. Commun. 47 (2009) 7419–7421.
[18] Y.X. Jiang, X.H. Fang, C.L. Bai, Signaling aptamer/protein binding by a molecular light switch complex, Anal. Chem. 76 (2004) 5230–5235.
[19] J. Wang, Y.X. Jiang, C.S. Zhou, X.H. Fang, Aptamer-based ATP assay using a luminescent light switching complex, Anal. Chem. 77 (2005) 3542–3546.
[20] X. Xiang, L. Chen, Q.G. Zhuang, X.H. Ji, Z.K. He, Real-time luminescence-based colorimetric determination of double-strand DNA in droplet on demand, Biosens. Bioelectron. 32 (2012) 43–49.
[21] C.H. Chen, X. Xiang, Y.F. Liu, G.H. Zhou, X.H. Ji, Z.K. He, Dual-color determination of protein via terminal protection of small-molecule-linked DNA and the enzymolysis of exonuclease III, Biosens. Bioelectron. 58 (2014) 205–208.
[22] R. Zhang, D.X. Zhao, H.G. Ding, Y.X. Huang, H.Z. Zhong, H.Y. Xie, Sensitive single-color fluorescence off–on switch system for dsDNA detection based on quantum dots–ruthenium assembling dyads, Biosens. Bioelectron. 56 (2014) 51–57.
[23] W.L. Sun, T.M. Yao, S. Shi, A molecular light switch Ru complex and quantum dots for the label-free, aptamer-based detection of thrombin, Analyst 137 (2012) 1550–1552.
[24] W.L. Sun, J.L. Yao, T.M. Yao, S. Shi, Label-free fluorescent DNA sensor for the detection of silver ions based on molecular light switch Ru complex and unmodified quantum dots, Analyst 138 (2013) 421–424.
[25] Y.L. Cao, S. Shi, L.L. Wang, J.L. Yao, T.M. Yao, Ultrasensitive fluorescence detection of heparin based on quantum dots and a functional ruthenium polypyridyl complex, Biosens. Bioelectron. 55 (2014) 174–179.
[26] Y.F. Liu, M. Luo, J. Yan, X. Xiang, X.H. Ji, G.H. Zhou, Z.K. He, An ultrasensitive biosensor for DNA detection based on hybridization chain reaction coupled with the efficient quenching of a ruthenium complex to CdTe quantum dots, Chem. Commun. 49 (2013) 7424–7426.
[27] Y.P. Zeng, J. Hu, Y. Long, C.Y. Zhang, Sensitive detection of DNA methyltransferase using hairpin probe-based primer generation rolling circle amplification-induced chemiluminescence, Anal. Chem. 85 (2013) 6143–6150.
[28] F.A. Wang, C.H. Lu, X.Q. Liu, L. Freage, I. Willner, Amplified and multiplexed detection of DNA using the dendritic rolling circle amplified synthesis of DNAzyme reporter units, Anal. Chem. 86 (2014) 1614–1621.
[29] A.P. Cao, C.Y. Zhang, Sensitive and label-free DNA methylation detection by ligation-mediated hyperbranched rolling circle amplification, Anal. Chem. 84 (2012) 6199–6205.
[30] E. Amouyal, A. Homsi, J.C. Chambron, J.P. Sauvage, Synthesis and study of a mixed-ligand ruthenium (II) complex in its ground and excited states: bis(2,2′-bipyridine)(dipyrido [3,2-a:2′,3′-c] phenazine-N^4N^5) ruthenium (II), J. Chem. Soc. Dalton Trans. (1990) 1841–1845.
[31] D. Zhao, Y. Fang, H.Y. Wang, Z.K. He, Synthesis and characterization of high-quality water-soluble CdTe: Zn^{2+} quantum dots capped by *N*-acetyl-L-cysteineviahydrothermal method, J. Mater. Chem. 21 (2011) 13365–13370.
[32] C.Q. Lin, Y.X. Zhang, X. Zhou, B. Yao, Q. Fang, Naked-eye detection of nucleic acids through rolling circle amplification and magnetic particle mediated aggregation, Biosens. Bioelectron. 47 (2013) 515–519.
[33] S.F. Liu, Y. Lin, L. Wang, T. Liu, C.B. Cheng, W.J. Wei, B. Tang, Exonuclease III-aided autocatalytic DNA biosensing platform for immobilization-free and ultrasensitive electrochemical detection of nucleic acid and protein, Anal. Chem. 86 (2014) 4008–4015.
[34] W.J. Zhou, X. Gong, Y. Xiang, R. Yuan, Y.Q. Chai, Quadratic recycling amplification for label-free and sensitive visual detection of HIV DNA, Biosens. Bioelectron. 55 (2014) 220–224.